Perspective

Black holes up close

https://doi.org/10.1038/s41586-023-05768-4

Received: 24 September 2022

Accepted: 27 January 2023

Published online: 22 March 2023

Check for updates

Ramesh Narayan[1,2]✉ & Eliot Quataert[3]

Recent developments have ushered in a new era in the field of black-hole astrophysics, providing a direct view of the remarkable environment near black-hole event horizons. These observations have enabled astronomers to confirm long-standing ideas on the physics of gas flowing into black holes with temperatures that are hundreds of times greater than at the centre of the Sun. At the same time, the observations have conclusively shown that light rays near a black hole experience large deflections that cause a dark shadow in the centre of the image, an effect predicted by Einstein's theory of general relativity. With further investment, this field is poised to deliver decades of advances in our understanding of gravity and black holes through stringent tests of general relativity, as well as insights into the role of black holes as the central engines powering a wide range of astronomical phenomena.

Einstein's theory of general relativity (GR) radically altered our understanding of the nature of space and time. In GR, space and time are dynamical quantities, leading to the existence of gravitational waves and the expanding Universe. But perhaps most remarkably, GR predicts a fundamentally new type of object, the black hole (BH). Unlike normal stars and planets that have surfaces, BHs in GR are defined by the presence of an event horizon, a region within which gravity is so strong that nothing can escape[1–3]. (There were Newtonian physics-based predictions of BH-like objects in the late 1700s by Michell[4] and Laplace[5], but their prescient ideas were too far ahead of the times and were not subsequently developed).

Although BHs (much like gravitational waves) were initially regarded as mathematical curiosities or even artefacts, starting in the 1960s BHs became a focus of research in both physics and astronomy[6,7].

In physics, BHs have played a central role in the theoretical quest for a quantum theory of gravity, in part because GR predicts its own failure in the interior of BHs: all of the matter out of which the BH is made collapses to a singularity of infinite density where the equations of GR break down. (Roger Penrose received a share of the 2020 Nobel Prize in Physics for his seminal paper[8] showing that such singularities generically form during gravitational collapse). There are also major theoretical puzzles in reconciling quantum mechanics and GR. The most traction in elucidating this tension has occurred in the context of understanding Hawking's famous prediction[9] that in quantum mechanics BHs should actually produce a small amount of radiation (which, we note, is completely unobservable for any BH that has been discovered).

In astronomy, a 60-year quest has led to the amazing realization that BHs are not only real but also commonplace. There are tens of millions of stellar-mass BHs per galaxy: a few of these happen to shine as bright X-ray sources, and gravitational-wave measurements have detected dozens of mergers of stellar-mass BHs. In addition, right at the centre of each galaxy, there is usually a supermassive BH with a mass of about 10^5–$10^{10}\,M_\odot$ (where $M_\odot \approx 1.99 \times 10^{33}$ g is the mass of the Sun).

Since the earliest discovery of BHs as quasars (enigmatic radio and optical sources at the centres of galaxies[10,11]), the quest was on to directly see the environment near the event horizon. In the most opportune cases, theorists predicted that such images would be dramatic[12,13]: a deficit of radiation from near the event horizon due to the strong bending of light by the BH's gravity, together with asymmetries in the image because half the radiating matter near the BH would be moving towards us (and thus appear brighter due to the special relativistic Doppler shift) and half would be moving away from us (and thus appear fainter). As shown in Fig. 1, those predictions have now been confirmed[14,15]. In particular, seeing the dark 'shadow' at the centre of the image and the ring of emission around it is a remarkable achievement that shows that our GR-inspired understanding of BHs is fundamentally correct.

Making these images was, however, extraordinarily challenging: it required a telescope with a thousand times better angular resolution than the James Webb Space Telescope and was akin to taking a picture of a tennis ball on the Moon using a camera on Earth. Many decades of theoretical, telescope and software development led to these remarkable results. We now provide additional context for understanding event-horizon-scale physics, what observations have been made so far and what the future may hold.

Black-hole accretion and gravity

This Perspective focuses primarily on two of the most well studied supermassive BHs: the 4×10^6-$M_\odot$ BH, called Sagittarius A* (Sgr A*), at the centre of our own Galaxy[16–20], and the approximately 6×10^9-$M_\odot$ BH, called M87* (ref. [21]), at the centre of the galaxy M87. The case for Sgr A* being a BH, based on measurements of the orbits of surrounding stars, is beyond a reasonable doubt; Reinhard Genzel and Andrea Ghez received a share of the 2020 Nobel Prize in Physics for this work. Observations of stars orbiting Sgr A* have also provided new tests of GR[22–25]. For our purposes here, Sgr A* and M87* are important primarily because they are nearby by astronomical standards, enabling particularly detailed studies (Fig. 1). (Although M87* is about 2,000 times farther away than Sgr A*, the event horizons of the two BHs subtend similar angles on the sky because of the much larger BH mass in M87*).

The most widely used technique to study BHs is seemingly paradoxical: contrary to their name, BHs are the central engines for some of the brightest and most unusual sources of radiation in the Universe. Astronomers use this radiation to study in detail these fascinating

[1]Center for Astrophysics, Harvard & Smithsonian, Cambridge, MA, USA. [2]Black Hole Initiative, Harvard University, Cambridge, MA, USA. [3]Department of Astrophysical Sciences, Princeton University, Princeton, NJ, USA. ✉e-mail: rnarayan@cfa.harvard.edu

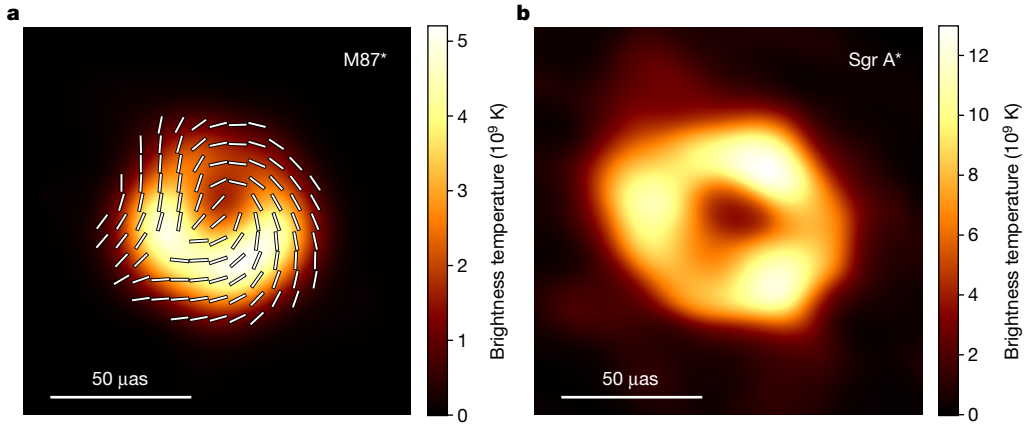

Fig. 1 | Event Horizon Telescope images of two supermassive BHs. a, Image of M87*. The colour scale corresponds to the 'brightness temperature' of the observed radiation and the tick marks indicate the orientation of linear polarization. **b**, Image of Sgr A*. Both images show a dark central region, called the 'shadow' of the BH, and an asymmetric ring of emission around it. Credit: D. Palumbo, adapted from published EHT results: ref. [91] under a Creative Commons licence CC BY 3.0; and refs. [92,93] under a Creative Commons licence CC BY 4.0.

objects. The radiation is produced by gas (outside the event horizon) that is spiralling into the BH via an accretion disk. Accretion converts gravitational potential energy into heat, which in turn can be converted into radiation and outflows of gas; BHs power the most spectacular observational sources via accretion because they have the strongest gravity of any object in the Universe. Indeed, the energy liberated by gas falling into supermassive BHs at the centres of galaxies can be so large that it strongly influences the formation of the host galaxy in which the BH resides[26]. BHs have thus become a central ingredient in our understanding of how the Universe evolved from the simplicity of the Big Bang to the dizzying variety of stars, planets and galaxies we see today[27–29]. The birth and growth of supermassive BHs in the first billion years after the Big Bang remains a major puzzle; new observational facilities, such as the James Webb Space Telescope, are likely to shed light on this longstanding problem.

Accretion disks around BHs are a major focus of research in astronomy. They involve rich physics including a complicated interplay of relativity, gravity, plasma physics, hydrodynamics, and electricity and magnetism. BH accretion disks, and their associated mass ejections in the form of relativistic jets, emit radiation across the entire electromagnetic spectrum, from radiowaves to gamma-rays, and are likely sources of high-energy neutrinos and cosmic rays. Much of the radiation we observe originates close to the event horizon, where most of the gravitational potential energy of the inflowing matter is released. As a result, accretion disks around BHs are also one of our best tools for studying physics in strong gravity, where manifestations of GR are expected to be most prominent.

Gas pulled in by a supermassive BH will typically carry substantial angular momentum (that is, a sense of rotation), which will prevent the gas from falling directly into the hole. However, magnetic-field lines embedded in the plasma can transfer angular momentum between fluid parcels. This enables gas to lose angular momentum and to spiral in towards the centere via an accretion disk[30]. A large fraction of the gravitational potential energy released by accretion is converted to heat (this is inevitable because of the 'friction' associated with angular momentum transfer), and thence to the radiation we observe (this last step is more tricky than one might think).

In a luminous system like a quasar, the conversion of heat to radiation is straightforward. As gas flows in, at each radius it self-consistently heats up to just the temperature needed to radiate away the added heat. As the gas approaches the BH, it reaches a temperature of about 10^5 K for a supermassive BH and of about 10^7 K for a stellar-mass BH. The former temperature leads to radiation primarily in the optical and ultraviolet bands, just like we observe in quasars, and the latter gives X-rays, as in the brightest stellar-mass BHs. In this 'standard' disk model[31,32], the radiation emitted at each radius is roughly of blackbody form, and the total luminosity of the accretion disk is about $0.1\dot{M}c^2$, where $\dot{M}$ is the mass accretion rate (grams per second) into the BH and c is the speed of light. The net result is that about 10% of the rest mass energy of the accreting gas is converted to radiation, which makes such an accretion disk far more efficient than the best nuclear power sources we have on Earth (about 0.1% conversion for a fission reactor and, theoretically, about 1% for a maximally efficient fusion reactor).

Hot accretion

In astrophysics, an important property associated with an object of mass M is its Eddington luminosity, $L_{\rm Edd} = 10^{38}(M/M_\odot)$ erg s^{-1}. This is the limiting luminosity at which the outwards push on a parcel of ionized gas by radiation just balances the inwards pull of gravity. The quasars and X-ray-bright BHs mentioned earlier have luminosities between a few per cent and 100% of $L_{\rm Edd}$.

Already in the 1970s it was clear that something strange happens with BH accretion when the luminosity falls below about 1% of $L_{\rm Edd}$. Stellar-mass BHs no longer radiate like 10^7-K blackbodies, but instead have much hotter gas with a temperature $T \approx 10^9$ K (ref. [33]). Supermassive BHs similarly change in character. They become unusually dim relative to the mass available for accretion[34], and they do not radiate like 10^5-K blackbodies[35]. Notably, Sgr A* produces hardly any radiation in any of the expected bands for a standard disk[36,37]; it is extremely dim, but at the same time appears to have gas at $T \approx 10^{10}$ K (refs. [38,39]). The problem was determining how an accretion disk can be hugely hotter than a standard disk and yet have a lower (sometimes far lower) luminosity. The solution to this problem lay in the identification of a very different mode of accretion called 'hot accretion'[40].

The initial breakthrough came with the recognition that it is possible to have a hot accretion model if the accreting material consists of a two-temperature plasma, a gas in which electrons are much cooler than ions (here 'ion' refers to the ionized nucleus of an atom, in practice, mostly ionized hydrogen, that is, protons). A two-temperature model of accretion was first developed in a seminal 1976 paper by Shapiro et al.[41]. In this model, as ions are too massive to radiate, they retain most of their viscous heat, reaching temperatures close to the virial temperature, $T \approx 10^{12}$ K near the BH. The pressure associated with this large ion temperature maintains the gas in a tenuous low-density state. The low density in turn ensures that thermal coupling between ions and electrons via Coulomb collisions (the electric force) is weak, thus allowing the plasma to retain its two-temperature character. The

electrons meanwhile radiate the energy they receive directly through viscous heat or by Coulomb collisions with the ions; the latter isn't much because of the low density. The low density also makes the gas relatively transparent to its own radiation, and this allows the system to avoid radiating like a blackbody. Overall, the model appears to be just what is needed to explain Sgr A*, M87* and a host of other low-luminosity BHs. Unfortunately, it has a fatal flaw: it is thermally unstable[42,43], which means that the system cannot survive for any length of time.

The next crucial breakthrough came with the recognition that there are in fact two different two-temperature hot accretion solutions, one being the above thermally unstable model and a second that is stable. The existence of two distinct hot solutions was first recognized by Ichimaru in a forgotten 1977 paper[44], with related ideas in later work[45]; it was then rediscovered in the 1990s[46–48] and developed in detail. The stable second solution underlies most current models of hot accretion[40,49]. One of its features is that the net radiative luminosity of the accretion disk is less than, often much less than, $0.1\dot{M}c^2$. These hot accretion solutions are thus described as being radiatively inefficient.

The first object for which a quantitative hot accretion model was developed was Sgr A* (ref. [50]). This early model predicted ion and electron temperatures near the BH of $T_i \approx 10^{12}$ K and $T_e \approx (1.1-1.3)\times 10^{10}$ K, respectively, and a very low radiative efficiency, $L/\dot{M}c^2 \approx 0.0004$. A year later, a similar model was developed for M87* (ref. [51]), with $T_e \approx 2\times 10^9$ K and radiative efficiency of about 0.001. In the years since, the hot accretion model has been the mainstay of this field, not only for Sgr A* and M87* but also for all low-luminosity supermassive and stellar-mass BHs (which are by far the dominant class of accreting BHs in the Universe)[35,40].

Although the hot accretion model is consistent with available observations, we should bear in mind that it is not necessarily correct. The model requires the key assumption of a two-temperature plasma, with outrageously hot ion and electron temperatures, hundreds of times hotter than the centre of the Sun in the case of electrons and yet another factor of hundred hotter for ions. Magnetized plasmas are known to have numerous microscopic instabilities, many with rapid growth rates. It is hard to believe that none of these instabilities is able to tap into the free energy associated with the vastly different ion and electron temperatures and drive the plasma to a single temperature. If even one instability were to succeed in equilibrating the ion and electron temperatures, a key foundation of the hot accretion scenario would collapse, and the entire model would cease to be viable. As we describe in the next section, recent observations have provided further support for the two-temperature hot accretion model and have allayed some of the doubts.

Inward bound

Two observational developments have provided a close-up view of the near-horizon environment of Sgr A* and M87*. The first is the continued progress of long-baseline interferometry, in the incarnation of the Event Horizon Telescope (EHT)[14]. The EHT is a set of radio telescopes spread across the Earth that can operate as a single instrument by collecting and storing the full electric-field information of the radiation as it hits the telescopes. This technique, interferometry[52], allows the resulting array of telescopes to obtain an angular resolution of λ/D, where λ is the wavelength of the radiation and D is the distance between pairs of telescopes. Fortuitously, for D comparable to the diameter of the Earth and $\lambda \approx 1$ mm (the shortest radio wavelength where Earth's atmosphere does not inhibit such observations), the resulting angular resolution is just sufficient to see event-horizon-scale structure in M87* and Sgr A*. Equally fortuitously, M87* and Sgr A* emit copious radiation at millimetre wavelengths so the sources are conveniently bright at just the wavelength where horizon-scale observations can be made. Finally, if these objects possess the kind of hot accretion flow suggested by models, then the gas would be relatively transparent at $\lambda \approx 1$ mm, which means that we can look all the way down to the BH horizon without any obscuration by the accreting gas.

The second key observational development is the GRAVITY interferometer, in which the European Southern Observatory's four 8-m Very Large Telescopes (VLTs) operate as an interferometer, creating images with ten-times-higher angular resolution than any single VLT alone could produce[53]. GRAVITY observes in the infrared at $\lambda = 2$ μm and has made spectacular contributions to our understanding of the Galactic Centre, including precise measurements of the BH mass and confirmation of GR via the precession of the orbit of the star S2 around the BH[25]. Unlike the EHT, the GRAVITY interferometer cannot directly resolve event-horizon-scale structure. Instead, however, it measures the position of the centre of light to an accuracy comparable to that of the size of the event horizon.

Figure 1 shows the EHT images of M87* and Sgr A*. The general features of these images are remarkably consistent with theoretical predictions made well before the observations: a deficit of light at small radii in the shadow region of the image[13], surrounded by a somewhat asymmetric bright ring of emission. Two primary constraints need to be satisfied to explain the EHT results. The first is that the radiation from the accreting gas must be produced within a region at most a factor of a few larger in size than the event horizon. In this case, the combined effects of the gravitational bending of light, which produces the shadow, and Doppler shifts due to the high speed of the gas, which produces the asymmetry in the ring, robustly produce images like those observed. The second constraint is that to explain the relatively modest azimuthal asymmetry around the ring, we must be viewing the rotating gas somewhat face-on, so that most of its orbital motion is not directed towards the observer at Earth. This is not surprising for M87*, in which there is independent evidence for such a viewing angle[54]. For Sgr A*, however, the implication is that the gas flowing into the BH has a sense of rotation that is somewhat orthogonal to that of the Galaxy as a whole. Earlier, the GRAVITY interferometer had provided evidence for just such a viewing angle. A few times a day, the BH in our Galactic Centre undergoes dramatic 'flares' in which the infrared and X-ray fluxes can increase by a factor of about 10–100 in less than an hour[55–57]. During one such flare, GRAVITY observed motion of the centre of light of the infrared emission suggestive of gas orbiting near the BH[58]. To cleanly see such orbital motion on the sky requires a viewing angle closer to face-on than edge-on, similar to that favoured by the EHT data.

Although the images in Fig. 1 viscerally convey the literally light-warping environment near a BH, the most detailed constraints on theoretical models of accretion physics come not from the images of total flux but rather from the polarization of the observed radiation. The millimetre and infrared emission observed in Sgr A* and M87* is synchrotron radiation, produced by energetic electrons spiralling around magnetic-field lines. Such radiation is predominantly linearly polarized, with the direction of polarization emitted by the plasma perpendicular to the local magnetic-field direction. Observations of the polarized radiation by the EHT and GRAVITY are so constraining because the polarization directly provides information about the magnetic-field direction near the event horizon, and because the polarization direction is also influenced by the plasma through propagation effects that modify the polarization in a density- and temperature-dependent manner.

Quantitatively interpreting many features of the EHT and GRAVITY data requires comparing theoretical models of the expected radiation to the observations. In doing so, the community relies primarily on numerical models of plasma flowing into a BH (see Fig. 2 for an example). Such models solve the equations for a magnetized fluid in the spacetime of a rotating BH[59,60]. The simulations then predict the temperature, magnetic-field strength, density of gas and so on as a function of space and time. Models of radiation produced by the plasma together with solutions to the transport of photons from the vicinity of the BH to a distant observer are then used to construct synthetic data for comparison with observations (we note that the techniques to make

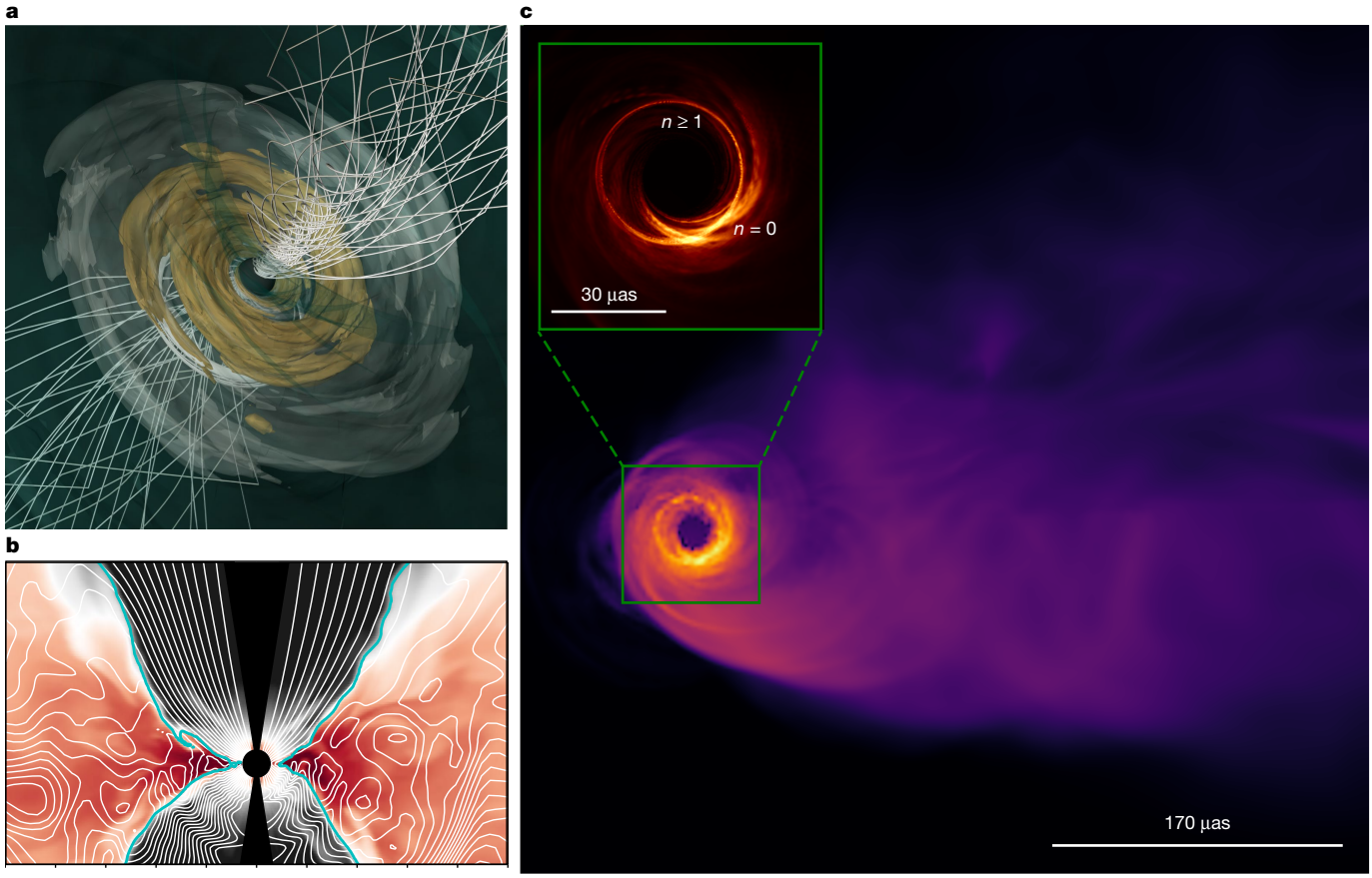

Fig. 2 | Numerical simulation of BH accretion and the resulting theoretically predicted image. a, Three-dimensional rendering of the magnetic field (white lines) and accretion disk, showing the twisting of magnetic-field lines in the jet due to the rotation of the BH. **b**, Edge-on view of gas density (red, high density; black, low density) and magnetic field (white lines) in a GR simulation of gas accreting onto a rotating BH. **c**, Theoretically predicted synchrotron image for M87* using the simulated plasma properties. The inset shows the brightness of radiation on a linear scale similar to current EHT data (with subrings defined in Fig. 3 labelled with integer *n*), whereas the main figure shows brightness on a logarithmic scale appropriate for future millimetre interferometers; the latter can directly reveal the connection between the near-horizon environment and the jet powered by BH rotation. Credit: A. Chael and G. Wong.

these predictions were developed well before the EHT observations[61,62]). There are some uncertain ingredients in such models, for example, how the simulations treat the electron versus proton temperature, what the structure of gas flowing towards the BH at large distances is and so on. Nonetheless, the theoretically favoured set of assumptions before the EHT observations have been remarkably successful at explaining most of the observational results.

Notably, a key conclusion of the theoretical modelling of EHT data on Sgr A* is that it is very hard to reconcile a single-temperature model with the observations; the plasma is very likely two-temperature[63]. We do not yet have a direct measurement of the ion temperature, so this conclusion is model dependent. Nevertheless, the EHT results now put the two-temperature hot accretion model on a firmer footing.

On a more quantitative note, the observed 'brightness temperature' (shown by the colour scale in Fig. 1) in the EHT images of Sgr A* and M87* correspond to electron temperatures $T_e > 1.3 \times 10^{10}$ K in Sgr A* and $T_e > 5 \times 10^9$ K in M87*, close to the values predicted by models developed a quarter of a century ago. (The measured brightness temperature is a lower limit on the electron temperature; in the case of Sgr A* and M87*, the electron temperature is probably a factor of a few larger than the brightness temperature).

The detailed comparison of theoretical models with observations also constrains the accretion rate $\dot{M}$ onto the BH, because the accretion rate sets the density and magnetic-field strength in the gas and thus many properties of the observed radiation. For Sgr A*, in particular, the inferred $\dot{M}$ (ref. [64]) is consistent with theoretical inferences made over two decades ago on the basis of the first detections of linear polarization in the millimetre radiation[65,66]. The current EHT-favoured models of Sgr A* and M87* have radiative efficiencies of about 10^{-3} and about 10^{-2}, respectively, again surprisingly close to long-ago predictions. Especially in Sgr A*, most of the accretion energy apparently goes through the horizon, rather than emerging as radiation. That is, the hot accretion flow in Sgr A* is radiatively inefficient, as predicted.

Testing gravity with the EHT

The region close to a BH and just outside the event horizon is where manifestations of GR are strongest and where gravity deviates the most from Newtonian physics. Here curvature of spacetime becomes extreme, space is 'dragged' by the BH's spin and the quintessential defining feature of a BH, its event horizon, forms. The EHT, with its ability to make images of this region, allows us an unprecedented opportunity to study GR. There are few quantitative probes of matter and spacetime under the strong-field conditions near a BH, so observationally diagnosing the near-horizon environment via interferometry is a remarkable opportunity to better understand the predictions of GR. In principle, such observations could also reveal hints of the new physics required by the incompatibility of GR and quantum mechanics.

We begin by discussing the event horizon. If Sgr A* or M87* were to possess a traditional surface rather than an event horizon, one might

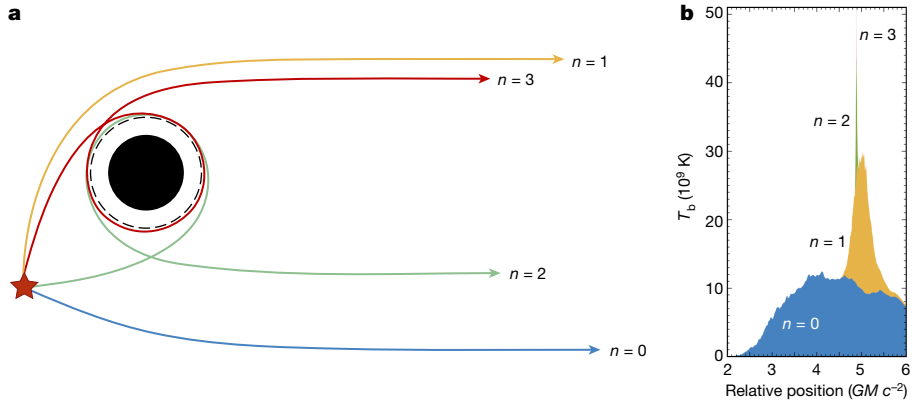

Fig. 3 | The origin of photon subrings. a, The path of light rays from a single emitting point traced forwards in GR to an observer at the far right. The light trajectories are labelled by the integer number n of half-orbits the photons undergo around the BH. Adding the contribution from all radiating plasma, the observer sees an image consisting of a concentric set of rings; the $n = 0$ rays will produce a relatively broad diffuse ring, whereas the $n = 1$ and higher rings will be progressively sharper (Fig. 2). **b**, Brightness temperature (T_b) in the image as a function of position (this is a theoretical zoom-in on the brightness near the rings in Fig. 1); the projected location of the centre of the BH is at an x-axis position of 0 in this figure, where the flux is very small (corresponding to the dark 'shadow' in Fig. 1). The different subrings in the image, corresponding to the trajectories in **a**, are labelled. The observed properties of the $n \geq 2$ subrings are determined primarily by GR, relatively independent of the accretion flow properties. At the current EHT resolution, what we observe is dominated by the direct $n = 0$ image, which has most of the flux, along with some contribution from $n = 1$ (Fig. 2). Future observations will be able to quantitatively determine the structure of the $n > 0$ rings, providing a strong test of GR. G, Newton's gravitational constant; M, mass of the BH. Credit: G. Wong (panel **b**).

expect some of the millimetre-wavelength radiation emitted by the accretion flow to bounce off the surface and to produce a visible feature precisely in the dark-shadow region of the images in Fig. 1. The absence of such a feature in current EHT images already rules out certain kinds of surfaces, and the constraints will become tighter in the future. More generally, any surface would absorb the thermal and mechanical energy dumped on it by the hot accretion flow and would re-radiate this energy. By combining EHT observations with infrared constraints from GRAVITY and other instruments, very strong limits can be put on such surface radiation, making it increasingly probable that Sgr A* and M87* have event horizons and are thus true BHs[67].

Moving on to spacetime curvature outside the horizon, this is physically parameterized by the metric, a mathematical construct that describes the geometry of spacetime. GR predicts a unique form for this metric—the Kerr metric[2]—with only two parameters: M, the mass of the BH, and a_*, a dimensionless number between 0 and 1 that quantifies the spin of the BH. (In principle, a third parameter, Q, the electric charge of the BH, is allowed[68], but astrophysical BHs are unlikely to have large enough Q to make a difference[69]). The prediction of GR that a BH is fully described by just two numbers makes a BH fundamentally different from any other type of astronomical object; for example, to describe a planet requires specifying its mass, rotation, radius, number of mountains, atmospheric properties, how big the oceans are and so on. A demonstration that the spacetime near a BH is perfectly described by the Kerr metric, and that no additional terms are present in the metric, is the holy grail of classical GR. The EHT has now brought us substantially closer to achieving this goal.

At first sight, it would appear that the predicted signatures of gravity in the observed image of an accreting BH would be inextricably lost in the complicated and not-fully-understood details of the accretion process. Fortunately, this is not the case. GR predicts that there are unique signatures of strong gravity in the image[12,70,71]. Gravitational bending of light is so strong around a BH that there is a characteristic radius, the photon orbit, at which even light must travel in a circular orbit around the BH. For radiation emitted by plasma close to the BH, GR predicts that some of the light in the image ends up in 'subrings' characterized by an integer n: the number of times the light undergoes half of a roughly circular orbit around the BH (Fig. 3). Remarkably, the sizes and shapes of the subrings are determined entirely by the metric; the only role of accretion is to light up these features for us to make observations. Thus, the subrings provide a direct map of the metric.

One worry is that the various subrings in the image overlap and the $n > 0$ subrings carry only a small fraction of the total flux. (In fact, the higher-order subrings, which are the cleanest probes of the metric, have exponentially suppressed fluxes). Fortunately, this does not make the entire enterprise impractical. In a brilliant insight, Johnson and Lupsasca[72] showed that interferometry separates out the signals from different subrings and places them in different and easily distinguished regions of data space (specifically, in different interferometric baselines). This allows us the opportunity to study subrings individually despite their low fluxes.

There are a number of proposals for precisely testing the Kerr nature of the BHs in Sgr A* and M87*. In the currently favoured accretion geometries, the shape of the dark shadow at the centre of the EHT images depends on both BH mass M and spin a_* so that a higher-fidelity image may allow both parameters of the BH to be independently measured, as well as any deviations of the spacetime from the Kerr metric to be searched for[67,73–75]. Measuring the shapes of the photon subrings is an even more robust approach as those features of the image depend solely on the spacetime, not the accretion flow structure[76,77].

The goal of testing the Kerr nature of the BH spacetime using astronomical observations of Sgr A* and M87* is incredibly exciting. It will undoubtedly require arrays with more telescopes (to see fainter features in the image) and higher angular resolution (to study the narrow photon subrings; Fig. 3). The latter is particularly challenging and requires going to either higher frequencies (where Earth's atmosphere does not cooperate) or longer baselines. Longer baselines will ultimately require satellites in space to resolve the $n \geq 2$ photon subrings.

Energy extraction from spinning BHs

In the popular imagination, a BH is an object that eats whatever it can lay its hands on and returns nothing to the external Universe. Although largely true, there is an important exception. In a penetratingly simple analysis, Penrose[78] showed that a spinning BH has free energy associated with its rotation that can be accessed from outside the hole. He described an explicit example involving particles in orbit around the

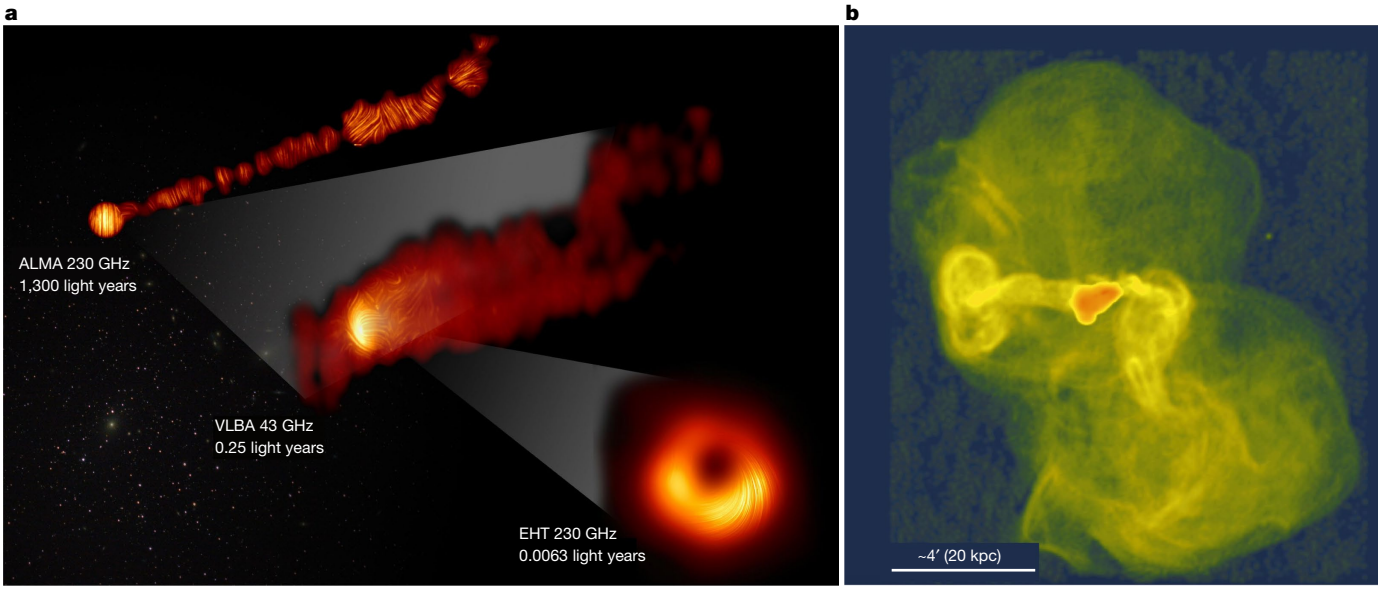

Fig. 4 | Radio and millimetre images of the relativistic jet in M87*. a, The three images[92,94,95] go from a scale of 0.006 light years in the EHT image at the bottom, which is similar to the size of the BH horizon, to a scale of 1,000 light years at the top, comparable in size to the core of the M87 galaxy. **b**, Large-scale image[96] that covers an area 100,000 light years across (kpc = 3,260 light years), showing that the jet stirs up a volume that includes the whole galaxy and beyond. Credit: left, EHT Collaboration; ALMA (ESO/NAOJ/NRAO), Goddi et al.; VLBA (NRAO), Kravchenko et al.; J. C. Algaba, I. Martí-Vidal; right, F. N. Owen, J. A. Eliek and N. E. Kassim, National Radio Astronomy Observatory, Associated Universities; reproduced with permission from ref. [96]; https://doi.org/10.1086/317151 (American Astronomical Society).

BH, which showed one way in which this energy might be extracted. The mechanism depends on frame dragging, the extraordinary prediction of GR that space exterior to a spinning object is dragged in the direction of rotation.

While the relevance of Penrose's particle-based toy example to astrophysics is unclear[79], a related mechanism that involves magnetic fields[69] looks very promising. Consider the magnetic-field configuration shown in Fig. 2a,b in which a bundle of magnetic-field lines is bunched around the rotation axis of a spinning BH. Because of frame dragging, the regions of these field lines close to the equatorial plane will be pulled around by the BH, whereas the same lines farther out will feel no such pull. This will induce spiral outgoing waves in the field lines, as in Fig. 2a, which will carry energy and angular momentum to large distances[80]. Correspondingly, the BH will spin down, losing angular momentum and mass energy.

Accreting BHs, especially of the supermassive variety, are well known for their relativistic jets: powerful collimated outflows of radiation and magnetized plasma moving out in twin oppositely directed beams at close to the speed of light. The prototypical example is M87*, which has a famous jet (Fig. 4) whose power exceeds the radiative power of the BH's accretion disk. The energy carried by such jets far away from the BH and into the surrounding galaxy turns out to be a major source of heating that strongly influences how the surrounding galaxy grows.

It is tempting to associate relativistic jets with the magnetic version of the Penrose process. Indeed, there is strong theoretical support for this proposal as computer simulations of hot accretion onto spinning BHs show that something similar to the observed jets forms spontaneously under fairly generic conditions[81]. Moreover, in some cases, the mechanical power in the simulated jet is larger than 100% of $\dot{M}c^2$, far larger than the 0.1% (for example, Sgr A*) or 1% (M87*) that comes out as radiation from a hot accretion disk, or even the approximately 10% (typical quasar) from a radiatively efficient standard disk. If the Penrose process is indeed the power source behind the multitude of relativistic jets found in the Universe, and if we could prove this, it would imply that rotating BHs all over the Universe are returning a part of their energy to the Universe, and that they are doing so by frame dragging, a central prediction of GR.

If we can prove specifically that the jet in M87* gets its power by bleeding spin energy from the BH, this would be a spectacular verification of frame dragging and the Penrose process. The combination of EHT images, polarization, and, better yet, videos based on time-resolved images, appears to be a promising tool to do this. For example, frame dragging probably imprints signatures on the shapes of polarized images, which may be observable in the future[82]. The harder step would be to show that frame dragging is the primary reason for the presence of the jet and that the energy actually flows out of the spinning BH.

Theoretical models indicate that the outflowing power in a jet powered by the magnetic version of the Penrose process depends on both the BH spin a_* and the amount of magnetic flux threading the BH horizon $\Phi_{\rm BH}$, with jet power $\propto a_*^2\,\Phi_{\rm BH}^2$ (refs. [69,81]). There is a limit to how rapidly a BH can spin; the limit corresponds to $a_* = 1$, which loosely speaking is when the horizon rotates at the speed of light. If there is not also a limit to how big $\Phi_{\rm BH}$ can grow, nature could make jets arbitrarily powerful by increasing $\Phi_{\rm BH}$ without bound. It turns out that there is in fact a limit on $\Phi_{\rm BH}$. If we try to squeeze more and more field lines close to the event horizon, the magnetic pressure builds up and pushes new lines away. The limiting magnetic flux is reached when the outwards push of the magnetic field just matches the inwards push of the accreting gas. A system in this limiting state is called a magnetically arrested disk (MAD). All other things being equal, a MAD system will have the most powerful jet. This maximum jet power is determined purely by the BH spin a_* and the mass accretion rate $\dot{M}$ (ref. [81]).

The models that successfully explain EHT observations of M87*, especially the polarization data (Fig. 1), require M87* to be in the MAD state[64]. This is consistent with the presence of a powerful jet in this system. GRAVITY- and EHT-based models indicate that Sgr A* also may be in the MAD state. Indeed, it is plausible that most hot accretion flows in the Universe are MAD, as once a system has reached the MAD limit, the field lines are pinned to the BH by the inflowing gas. The only way to eliminate the field is by bringing in magnetic flux of the opposite

sign and cancelling out what is already there. The new flux should have the precise magnitude to avoid under- or overshooting, which seems unrealistic.

Curiously, Sgr A* does not show any obvious sign of a jet. If this system is in the MAD state, as models suggest, then a plausible explanation for the lack of a powerful jet is that the BH spins very slowly. This hypothesis will be tested once the BH spin is measured. Alternatively, it could be that a jet is actually present[83–85] but is stifled by the surrounding environment, which prevents the jet from travelling to large distances from the BH where it could be more readily observed.

Looking forwards

In reflecting on the diverse science enabled by the initial EHT and GRAVITY results for Sgr A* and M87*, it is inspiring to realize that this is but a taste of what is to come. We are at the beginning of what will be a many decades journey to increasingly precise observations of the environment around BH event horizons. In the future, improved infrared interferometery and spectroscopy with bigger telescopes will detect stars even closer to the BH in Sgr A* and will better characterize the near-horizon environment via measurements of orbits and observations of flares. If we are lucky, we may discover a radio pulsar in orbit around Sgr A*; precision timing of this pulsar would be a game changer[86]. Future generations of millimetre interferometers, both on the ground and in space, will reveal far more details of the near-horizon environment. This will enable stringent tests of GR using the photon subrings. A second key advance will be directly observing emission farther from the BH, elucidating the connections between the accretion inflow, the (likely) spinning BH and the outflowing jet, all of which are critical for understanding the broader role of BHs in the formation of structure in the Universe.

In parallel to these advances in our understanding of BHs using light, observations of gravitational waves from merging BHs (a topic beyond the scope of this Perspective) will continue to improve dramatically. The timing of radio pulsars in our Galaxy is approaching the needed sensitivity to detect the gravitational-wave background produced by mergers of about 10^9-$M_\odot$ BHs[87]. Next-generation ground-based detectors will be able to observe stellar-mass BH mergers across the cosmos[88]; detailed studies of the brightest of these events will test the uniqueness of the Kerr BH solution. In the 2030s, the space-based Laser Interferometer Space Antenna (LISA) gravitational-wave observatory will be launched and will detect mergers of about $10^{5–7}$-$M_\odot$ binary BHs, as well as stellar-mass objects spiralling in towards a massive BH[89].

Data availability

EHT data for Fig. 1 are available at https://github.com/eventhorizontelescope.

Code availability

Figure 1 and the right panel of Fig. 2 were created using the ehtim (eht-imaging) software package[90] which is available at https://github.com/achael/eht-imaging.

1. Schwarzschild, K. On the gravitational field of a mass point according to Einstein's theory. *Abh. Konigl. Preuss. Akad. Wiss. Berlin* **1916**, 189–196 (1916).
2. Kerr, R. P. Gravitational field of a spinning mass as an example of algebraically special metrics. *Phys. Rev. Lett.* **11**, 237–238 (1963).
   An exact analytical solution of general relativity describing the most general spinning uncharged black hole.
3. Misner, C. W., Thorne, K. S. & Wheeler, J. A. *Gravitation* (Princeton Univ. Press, 2018).
4. Michell, J. On the means of discovering the distance, magnitude, &c. of the fixed stars, in consequence of the diminution of the velocity of their light, in case such a diminution should be found to take place in any of them, and such other data should be procured from observations, as would be farther necessary for that purpose. By the Rev. John Michell, B. D. F. R. S. in a letter to Henry Cavendish, Esq. F. R. S. and A. S. *Phil. Trans. R. Soc. Lond.* **74**, 35–57 (1784).
5. Laplace, P. S. Beweis des Satzes, dass die anziehende Kraft bey einem Weltkörper so groß seyn könne, dass das Licht davon nicht ausströmen kann. *Allg. Geogr. Ephemer.* **4**, 1–6 (1799).
6. Thorne, K. S. *Black Holes and Time Warps: Einstein's Outrageous Legacy* (W. W. Norton, 1994).
7. Begelman, M. & Rees, M. *Gravity's Fatal Attraction* (Cambridge Univ. Press, 2020).
8. Penrose, R. Gravitational collapse and space-time singularities. *Phys. Rev. Lett.* **14**, 57–59 (1965).
   Mathematical proof that black-hole formation is inevitable in general relativity from certain generic initial conditions.
9. Hawking, S. W. Particle creation by black holes. *Commun. Math. Phys.* **43**, 199–220 (1975).
10. Schmidt, M. 3C 273 : a star-like object with large red-shift. *Nature* **197**, 1040 (1963).
    Discovery that the quasar 3C 273, later identified as an accreting supermassive black hole, is at a redshift of 0.158 and therefore very distant from our Galaxy and highly luminous.
11. Salpeter, E. E. Accretion of interstellar matter by massive objects. *Astrophys. J.* **140**, 796–800 (1964).
12. Luminet, J.-P. Image of a spherical black hole with thin accretion disk. *Astron. Astrophys.* **75**, 228–235 (1979).
13. Falcke, H., Melia, F. & Agol, E. Viewing the shadow of the black hole at the Galactic Center. *Astrophys. J. Lett.* **528**, 13–16 (2000).
14. Event Horizon Telescope Collaboration First M87 Event Horizon Telescope results. I. The shadow of the supermassive black hole. *Astrophys. J. Lett.* **875**, 1 (2019).
    Landmark experiment with the Event Horizon Telescope that obtained the image of the supermassive black hole M87* and confirmed the predicted black-hole shadow.
15. Event Horizon Telescope Collaboration First Sagittarius A* Event Horizon Telescope results. I. The shadow of the supermassive black hole in the center of the Milky Way. *Astrophys. J. Lett.* **930**, 12 (2022).
16. Eckart, A. & Genzel, R. Observations of stellar proper motions near the Galactic Centre. *Nature* **383**, 415–417 (1996).
17. Ghez, A. M., Klein, B. L., Morris, M. & Becklin, E. E. High proper-motion stars in the vicinity of Sagittarius A*: evidence for a supermassive black hole at the center of our Galaxy. *Astrophys. J.* **509**, 678–686 (1998).
18. Ghez, A. M., Morris, M., Becklin, E. E., Tanner, A. & Kremenek, T. The accelerations of stars orbiting the Milky Way's central black hole. *Nature* **407**, 349–351 (2000).
    Measurement of the accelerations of stars orbiting the object Sagittarius A* at the centre of the Galaxy.
19. Schödel, R. et al. A star in a 15.2-year orbit around the supermassive black hole at the centre of the Milky Way. *Nature* **419**, 694–696 (2002).
    Landmark study that reported a nearly complete orbit of a star at the centre of our Galaxy and proved beyond reasonable doubt that Sagittarius A* is a four-million-solar-mass black hole.
20. Ghez, A. M. et al. Stellar orbits around the Galactic Center black hole. *Astrophys. J.* **620**, 744–757 (2005).
21. Gebhardt, K. et al. The Black Hole mass in M87 from Gemini/NIFS adaptive optics observations. *Astrophys. J.* **729**, 119 (2011).
22. Hees, A. et al. Testing general relativity with stellar orbits around the supermassive black hole in our Galactic Center. *Phys. Rev. Lett.* **118**, 211101 (2017).
23. GRAVITY Collaboration Detection of the gravitational redshift in the orbit of the star S2 near the Galactic Centre massive black hole. *Astron. Astrophys.* **615**, 15 (2018).
24. Do, T. et al. Relativistic redshift of the star S0-2 orbiting the Galactic Center supermassive black hole. *Science* **365**, 664–668 (2019).
25. GRAVITY Collaboration Detection of the Schwarzschild precession in the orbit of the star S2 near the Galactic Centre massive black hole. *Astron. Astrophys.* **636**, 5 (2020).
26. Di Matteo, T., Springel, V. & Hernquist, L. Energy input from quasars regulates the growth and activity of black holes and their host galaxies. *Nature* **433**, 604–607 (2005).
27. Brüggen, M. & Kaiser, C. R. Hot bubbles from active galactic nuclei as a heat source in cooling-flow clusters. *Nature* **418**, 301–303 (2002).
28. Cattaneo, A. et al. The role of black holes in galaxy formation and evolution. *Nature* **460**, 213–219 (2009).
29. Fabian, A. C. Observational evidence of active galactic nuclei feedback. *Annu. Rev. Astron. Astrophys.* **50**, 455–489 (2012).
30. Balbus, S. A. & Hawley, J. F. A powerful local shear instability in weakly magnetized disks. I. Linear analysis. *Astrophys. J.* **376**, 214–222 (1991).
31. Shakura, N. I. & Sunyaev, R. A. Black holes in binary systems. Observational appearance. *Astron. Astrophys.* **24**, 337–355 (1973).
32. Novikov, I. D. & Thorne, K. S. in *Black Holes (Les Astres Occlus)* (eds DeWitt, C. & DeWitt, B.) 343–450 (Gordon & Breach, 1973).
33. Esin, A. A., McClintock, J. E. & Narayan, R. Advection-dominated accretion and the spectral states of black hole X-ray binaries: application to Nova Muscae 1991. *Astrophys. J.* **489**, 865–889 (1997).
34. Fabian, A. C. & Canizares, C. R. Do massive black holes reside in elliptical galaxies? *Nature* **333**, 829–831 (1988).
35. Ho, L. C. Nuclear activity in nearby galaxies. *Ann. Rev. Astron. Astrophys.* **46**, 475–539 (2008).
36. Goldwurm, A. et al. Possible evidence against a massive black hole at the Galactic Centre. *Nature* **371**, 589–591 (1994).
37. Grindlay, J. E. Black holes take centre stage? *Nature* **371**, 561–562 (1994).
38. Krichbaum, T. P. et al. VLBI observations of the Galactic Center source SGR A* at 86 GHz and 215 GHz. *Astron. Astrophys.* **335**, 106–110 (1998).
39. Shen, Z.-Q., Lo, K. Y., Liang, M. C., Ho, P. T. P. & Zhao, J.-H. A size of ~1 AU for the radio source Sgr A* at the centre of the Milky Way. *Nature* **438**, 62–64 (2005).
40. Yuan, F. & Narayan, R. Hot accretion flows around black holes. *Ann. Rev. Astron. Astrophys.* **52**, 529–588 (2014).
41. Shapiro, S. L., Lightman, A. P. & Eardley, D. M. A two-temperature accretion disk model for Cygnus X-1: structure and spectrum. *Astrophys. J.* **204**, 187–199 (1976).

42. Pringle, J. E. Thermal instabilities in accretion discs. *Mon. Not. R. Astron. Soc.* **177**, 65–71 (1976).
43. Piran, T. The role of viscosity and cooling mechanisms in the stability of accretion disks. *Astrophys. J.* **221**, 652–660 (1978).
44. Ichimaru, S. Bimodal behavior of accretion disks: theory and application to Cygnus X-1 transitions. *Astrophys. J.* **214**, 840–855 (1977).
45. Rees, M. J., Begelman, M. C., Blandford, R. D. & Phinney, E. S. Ion-supported tori and the origin of radio jets. *Nature* **295**, 17–21 (1982).
46. Narayan, R. & Yi, I. Advection-dominated accretion: a self-similar solution. *Astrophys. J. Lett.* **428**, 13–16 (1994).
47. Narayan, R. & Yi, I. Advection-dominated accretion: underfed black holes and neutron stars. *Astrophys. J.* **452**, 710–735 (1995).
48. Abramowicz, M. A., Chen, X., Kato, S., Lasota, J.-P. & Regev, O. Thermal equilibria of accretion disks. *Astrophys. J. Lett.* **438**, 37–39 (1995).
49. Narayan, R., Mahadevan, R. & Quataert, E. in *Theory of Black Hole Accretion Disks* (eds Abramowicz, M. A. et al.) 148–182 (Cambridge Univ. Press, 1998).
50. Narayan, R., Yi, I. & Mahadevan, R. Explaining the spectrum of Sagittarius A* with a model of an accreting black hole. *Nature* **374**, 623–625 (1995).
Application of the hot-accretion-flow model to an astrophysical black hole, Sagittarius A* at our Galactic Centre.
51. Reynolds, C. S., Di Matteo, T., Fabian, A. C., Hwang, U. & Canizares, C. R. The 'quiescent' black hole in M87. *Mon. Not. R. Astron. Soc.* **283**, 111–116 (1996).
52. Thompson, A. R., Moran, J. M. & Swenson, G. W. *Interferometry and Synthesis in Radio Astronomy* 3rd edn (Springer, 2017).
53. Eisenhauer, F. et al. GRAVITY: getting to the event horizon of Sgr A*. In *Optical and Infrared Interferometry Society of Photo-Optical Instrumentation Engineers Conference Series* Vol. 7013 (eds Schöller, M. et al.) 70132 (SPIE, 2008).
54. Walker, R. C., Hardee, P. E., Davies, F. B., Ly, C. & Junor, W. The structure and dynamics of the subparsec jet in M87 based on 50 VLBA observations over 17 Years at 43 GHz. *Astrophys. J.* **855**, 128 (2018).
55. Baganoff, F. K. et al. Rapid X-ray flaring from the direction of the supermassive black hole at the Galactic Centre. *Nature* **413**, 45–48 (2001).
56. Genzel, R. et al. Near-infrared flares from accreting gas around the supermassive black hole at the Galactic Centre. *Nature* **425**, 934–937 (2003).
57. Ghez, A. M. et al. Variable infrared emission from the supermassive black hole at the center of the Milky Way. *Astrophys. J. Lett.* **601**, 159–162 (2004).
58. GRAVITY Collaboration Detection of orbital motions near the last stable circular orbit of the massive black hole SgrA*. *Astron. Astrophys.* **618**, 10 (2018).
Detection of looped clockwise motion of infrared-emitting gas around the Galactic Centre black hole Sagittarius A*.
59. Gammie, C. F., McKinney, J. C. & Tóth, G. HARM: a numerical scheme for general relativistic magnetohydrodynamics. *Astrophys. J.* **589**, 444–457 (2003).
60. De Villiers, J.-P. & Hawley, J. F. A numerical method for general relativistic magnetohydrodynamics. *Astrophys. J.* **589**, 458–480 (2003).
61. Mościbrodzka, M., Gammie, C. F., Dolence, J. C., Shiokawa, H. & Leung, P. K. Radiative models of SGR A* from GRMHD simulations. *Astrophys. J.* **706**, 497–507 (2009).
62. Dexter, J., Agol, E., Fragile, P. C. & McKinney, J. C. The submillimeter bump in Sgr A* from relativistic MHD simulations. *Astrophys. J.* **717**, 1092–1104 (2010).
63. Event Horizon Telescope Collaboration First Sagittarius A* Event Horizon Telescope results. V. Testing astrophysical models of the Galactic Center black hole. *Astrophys. J. Lett.* **930**, 16 (2022).
64. Event Horizon Telescope Collaboration First M87 Event Horizon Telescope results. VIII. Magnetic field structure near the event horizon. *Astrophys. J. Lett.* **910**, 13 (2021).
65. Agol, E. Sagittarius A* polarization: no advection-dominated accretion flow, low accretion rate, and nonthermal synchrotron emission. *Astrophys. J. Lett.* **538**, 121–124 (2000).
66. Quataert, E. & Gruzinov, A. Constraining the accretion rate onto Sagittarius A* using linear polarization. *Astrophys. J.* **545**, 842–846 (2000).
67. Event Horizon Telescope Collaboration First Sagittarius A* Event Horizon Telescope results. VI. Testing the black hole metric. *Astrophys. J. Lett.* **930**, 17 (2022).
68. Newman, E. T. et al. Metric of a rotating, charged mass. *J. Math. Phys.* **6**, 918–919 (1965).
69. Blandford, R. D. & Znajek, R. L. Electromagnetic extraction of energy from Kerr black holes. *Mon. Not. R. Astron. Soc.* **179**, 433–456 (1977).
Demonstration that magnetic fields threading the black-hole horizon can extract rotational energy of the black hole, powering relativistic jets.
70. Darwin, C. The gravity field of a particle. *Proc. R. Soc. Lond. Ser. A* **249**, 180–194 (1959).
71. Bardeen, J. M. in *Black Holes (Les Astres Occlus)* (eds DeWitt, C. & DeWitt, B.) 241–289 (Gordon & Breach, 1973).
72. Johnson, M. D. & Lupsasca, A. et al. Universal interferometric signatures of a black hole's photon ring. *Sci. Adv.* **6**, 1310 (2020).
Description of the formation of a set of nested self-similar subrings by black-hole lensing, and discussion of how the subrings could be disentangled in the image via interferometry.
73. Broderick, A. E., Johannsen, T., Loeb, A. & Psaltis, D. Testing the no-hair theorem with Event Horizon Telescope observations of Sagittarius A*. *Astrophys. J.* **784**, 7 (2014).
74. Psaltis, D. et al. Gravitational test beyond the first post-Newtonian order with the shadow of the M87 black hole. *Phys. Rev. Lett.* **125**, 141104 (2020).
75. Chael, A., Johnson, M. D. & Lupsasca, A. Observing the inner shadow of a black hole: a direct view of the event horizon. *Astrophys. J.* **918**, 6 (2021).
76. Johannsen, T. & Psaltis, D. Testing the no-hair theorem with observations in the electromagnetic spectrum. II. Black hole images. *Astrophys. J.* **718**, 446–454 (2010).
77. Gralla, S. E., Lupsasca, A. & Marrone, D. P. The shape of the black hole photon ring: a precise test of strong-field general relativity. *Phys. Rev. D* **102**, 124004 (2020).
78. Penrose, R. Gravitational collapse: the role of general relativity. *Nuovo Cimento Rivista Serie* **1**, 252 (1969).
79. Bardeen, J. M., Press, W. H. & Teukolsky, S. A. Rotating black holes: locally nonrotating frames, energy extraction, and scalar synchrotron radiation. *Astrophys. J.* **178**, 347–370 (1972).
80. Semenov, V., Dyadechkin, S. & Punsly, B. Simulations of jets driven by black hole rotation. *Science* **305**, 978–980 (2004).
81. Tchekhovskoy, A., Narayan, R. & McKinney, J. C. Efficient generation of jets from magnetically arrested accretion on a rapidly spinning black hole. *Mon. Not. R. Astron. Soc.* **418**, 79–83 (2011).
82. Ricarte, A., Palumbo, D. C. M., Narayan, R., Roelofs, F. & Emami, R. Observational signatures of frame dragging in strong gravity. *Astrophys. J. Lett.* **941**, L12 (2022).
83. Falcke, H. & Markoff, S. The jet model for Sgr A*: radio and X-ray spectrum. *Astron. Astrophys.* **362**, 113–118 (2000).
84. Yusef-Zadeh, F., Roberts, D., Wardle, M., Heinke, C. O. & Bower, G. C. Flaring activity of Sagittarius A* at 43 and 22 GHz: evidence for expanding hot plasma. *Astrophys. J.* **650**, 189–194 (2006).
85. Brinkerink, C. D., Falcke, H., Law, C. J., Barkats, D. & Bower, G. C. et al. ALMA and VLA measurements of frequency-dependent time lags in Sagittarius A*: evidence for a relativistic outflow. *Astron. Astrophys.* **576**, 41 (2015).
86. Psaltis, D., Wex, N. & Kramer, M. A quantitative test of the no-hair theorem with Sgr A* using stars, pulsars, and the Event Horizon Telescope. *Astrophys. J.* **818**, 121 (2016).
87. Arzoumanian, Z. et al. The NANOGrav 12.5 yr data set: search for an isotropic stochastic gravitational-wave background. *Astrophys. J. Lett.* **905**, 34 (2020).
88. Kalogera, V. et al. The next generation global gravitational wave observatory: the science book. Preprint at https://arxiv.org/abs/2111.06990 (2021).
89. Amaro-Seoane, P. et al. Laser Interferometer Space Antenna. Preprint at https://arxiv.org/abs/1702.00786 (2017).
90. Chael, A. A. et al. Interferometric imaging directly with closure phases and closure amplitudes. *Astrophys. J.* **857**, 23 (2018).
91. Event Horizon Telescope Collaboration First M87 Event Horizon Telescope results. IV. Imaging the central supermassive black hole. *Astrophys. J. Lett.* **875**, 4 (2019).
92. Event Horizon Telescope Collaboration First M87 Event Horizon Telescope results. VII. Polarization of the ring. *Astrophys. J. Lett.* **910**, 12 (2021).
93. Event Horizon Telescope Collaboration First Sagittarius A* Event Horizon Telescope results. III. Imaging of the Galactic Center supermassive black hole. *Astrophys. J. Lett.* **930**, 14 (2022).
94. Goddi, C. et al. Polarimetric properties of Event Horizon Telescope targets from ALMA. *Astrophys. J. Lett.* **910**, 14 (2021).
95. Kravchenko, E. et al. Linear polarization in the nucleus of M87 at 7 mm and 1.3 cm. *Astron. Astrophys.* **637**, 6 (2020).
96. Owen, F. N., Eilek, J. A. & Kassim, N. E. M87 at 90 centimeters: a different picture. *Astrophys. J.* **543**, 611–619 (2000).

Acknowledgements We thank A. Chael, D. Palumbo and G. Wong for their help making Figs. 1–3.

Author contributions R.N. and E.Q. contributed equally to all aspects of the paper.

Competing interests The authors declare no competing interests.

Additional information

Correspondence and requests for materials should be addressed to Ramesh Narayan.

Peer review information *Nature* thanks the anonymous reviewers for their contribution to the peer review of this work.